# Radiative Toroidal Dipole and Anapole Excitations in Collectively Responding Arrays of Atoms

K. E. Ballantine* and J. Ruostekoski†
*Department of Physics, Lancaster University, Lancaster LA1 4YB, United Kingdom*

(Received 12 May 2020; accepted 17 July 2020; published 4 August 2020)

A toroidal dipole represents an often overlooked electromagnetic excitation distinct from the standard electric and magnetic multipole expansion. We show how a simple arrangement of strongly radiatively coupled atoms can be used to synthesize a toroidal dipole where the toroidal topology is generated by radiative transitions forming an effective poloidal electric current wound around a torus. We extend the protocol for methods to prepare a delocalized collective excitation mode consisting of a synthetic lattice of such toroidal dipoles and a nonradiating, yet oscillating charge-current configuration, dynamic anapole, for which the far-field radiation of a toroidal dipole is identically canceled by an electric dipole.

DOI: 10.1103/PhysRevLett.125.063201

The concept of electric and magnetic multipoles vastly simplifies the study of light-matter interaction, allowing the decomposition both of the scattered light and of the charge and current sources [1,2]. While the far-field radiation can be fully described by the familiar transverse-electric and -magnetic multipoles, the full characterization of the current requires, however, an additional series that is independent of electric and magnetic multipoles: dynamic toroidal multipoles [3–6]. These are extensions of static toroidal dipoles [7] that have been studied in nuclear, atomic, and solid-state physics, e.g., in the context of parity violations in electroweak interactions [8–10] and in multiferroics [11]. Often obscured and neglected in comparison to electric and magnetic multipoles due to its weakness, the toroidal dipole can have an important response to electromagnetic fields in systems of toroidal geometry [12]. Dynamic toroidal dipoles are actively studied in artificial metamaterials that utilize such designs, with responses varying from the microwave to the optical part of the spectrum [13–18]. Crucially, an electric dipole together with a toroidal dipole can form a nonradiating dynamic anapole [19–22], where the far-field emission pattern from both dipoles interferes destructively, so the net emission is zero.

Light can mediate strong resonance interactions between closely spaced ideal emitters, and an especially pristine system exhibiting cooperative optical response is that of regular planar arrays of cold atoms with unit occupancy [23–36]. Subradiant linewidth narrowing of transmitted light has now been observed in such a system formed by an optical lattice [37]. In the experiment the whole array was collectively responding to light with the atomic dipoles oscillating in phase. Furthermore, the lattice potentials can be engineered [38], and a great flexibility of optical transitions is provided by atoms such as Sr and Yb [39]. Also several other experimental approaches exist to trap and arrange atoms with single-site control [40–46].

Here we propose how to harness strong light-mediated interactions between atoms to engineer collective radiative excitations that synthesize effective dynamic toroidal dipole and nonradiating anapole moments, even though individual atoms only exhibit electric dipole transitions. The method is based on simple arrangements of atoms, where the toroidal topology is generated by radiative transitions forming an effective poloidal electric current wound around a torus, such that an induced magnetization forms a closed circulation inside the torus. The toroidal and anapole modes can be excited by radially polarized incident light and, in the case of the anapole, with a focusing lens. The resulting anapole excitation shows a sharp drop in the far-field dipole radiation, despite having a large collective electronic excitation of the atoms associated with both electric and toroidal dipole modes. Such a configuration represents stored excitation energy without radiation that is fundamentally different, e.g., from subradiance [47]. We extend the general principle to larger systems, and show in sizable arrays how this collective behavior of atoms allows us to engineer a delocalized collective radiative excitation eigenmode consisting of an effective periodic lattice of toroidal dipoles. Such an array is then demonstrated to exhibit collective subradiance, with the narrow resonance line sensitively depending on the lattice spacing and manifesting itself as a Fano resonance in the coherently transmitted light.

Utilizing cold atoms as a platform for exploring toroidal excitation topology has several advantages, as it naturally allows for the toroidal response at optical frequencies, with emitters much smaller than a resonant wavelength, and avoids dissipative losses present in plasmonics or circuit resonators forming metamaterials. Moreover, the atomic arrangement can form a genuine quantum system, and our analysis is valid also in the single-photon quantum limit.

 

To demonstrate the formation of an effective toroidal dipole and anapole in an atomic ensemble, we briefly describe the radiative coupling between cold atoms. For simplicity of presentation, we analyze the coherently driven case, but the formalism is also valid in the quantum regime of single-photon excitations [48].

We consider atoms at fixed positions, with a $J=0\rightarrow J'=1$ transition, and assume a controllable Zeeman splitting of the $J'=1$ levels, generated, e.g., by a periodic optical pattern of ac Stark shifts [73]. The dipole moment of atom $j$ is $\mathbf{d}_j=\mathcal{D}\sum_j \mathcal{P}_\sigma^{(j)}\hat{\mathbf{e}}_\sigma$, where $\mathcal{D}$ denotes the reduced dipole matrix element, and $\mathcal{P}_\sigma^{(j)}$ and $\hat{\mathbf{e}}_\sigma$ the polarization amplitude and unit vector associated with the $|J=0, m=0\rangle\rightarrow|J'=1, m=\sigma\rangle$ transition, respectively. The collective response of the atoms in the limit of low light intensity [23,49–51,74,75] then follows from $\dot{\mathbf{b}}=i\mathcal{H}\mathbf{b}+\mathbf{f}$, where $\mathbf{b}_{3j-1+\sigma}=\mathcal{P}_\sigma^{(j)}$ and the driving $\mathbf{f}_{3j-1+\sigma}=i(\xi/\mathcal{D})\hat{\mathbf{e}}_\sigma^*\cdot\epsilon_0\boldsymbol{\mathcal{E}}(\mathbf{r}_j)$, with the incident light field of amplitude $\boldsymbol{\mathcal{E}}(\mathbf{r})=\mathcal{E}_0\hat{\mathbf{e}}_{\rm in}\exp(ikx)$ [76], polarization $\hat{\mathbf{e}}_{\rm in}$, and frequency $\omega=kc$. Here $\xi=6\pi\gamma/k^3$ depends on the single-atom linewidth $\gamma=\mathcal{D}^2k^3/(6\pi\epsilon_0\hbar)$. The matrix $\mathcal{H}$ describes interactions between different atoms due to multiple scattering of light, with $\mathcal{H}_{3j-1+\sigma,3k-1+\sigma'}=\xi\hat{\mathbf{e}}_\sigma^*\cdot\mathsf{G}(\mathbf{r}_j-\mathbf{r}_k)\hat{\mathbf{e}}_{\sigma'}$ for $(j,\sigma)\neq(k,\sigma')$, where the dipole radiation kernel $\mathsf{G}(\mathbf{r})$ gives the field $\epsilon_0\mathbf{E}_s^{(j)}(\mathbf{r})=\mathsf{G}(\mathbf{r}-\mathbf{r}_j)\mathbf{d}_j$ from a dipole moment $\mathbf{d_j}$ at $\mathbf{r}_j$ [1]. The diagonal element $\mathcal{H}_{3j+\sigma-1,3j+\sigma-1}=\Delta_\sigma^{(j)}+i\gamma$, where $\Delta_\sigma^{(j)}=\delta_\sigma^{(j)}+\Delta$ consists of an overall laser detuning $\Delta=\omega-\omega_0$ from the single-atom resonance $\omega_0$, plus a relative shift $\delta_\sigma^{(j)}$ of each level. The dynamics follows from the eigenvectors $\mathbf{v}_n$ and eigenvalues $\delta_n+i\gamma_n$ of $\mathcal{H}$ giving the collective level shifts $\delta_n$ and linewidths $\gamma_n$ [52].

The limit of low light intensity corresponds to linear regime of oscillating atomic dipoles. The analogous quantum limit is that of a single photon that experiences no nonlinear interactions, as at minimum, two simultaneous photons are required for interactions. Regarding one-body expectation values, the equations of motion for the dipole amplitudes $\mathcal{P}_\sigma^{(j)}$ are indeed precisely the same [53] as those for single-photon excitation amplitudes that are radiatively coupled between the atoms by $\mathcal{H}$ [48].

To illustrate the role of toroidal multipoles, we consider the far-field scattered light from a radiation source decomposed into vector spherical harmonics [1],

$$\mathbf{E}_s^{(j)}=\sum_{l=0}^{\infty}\sum_{m=-l}^{l}(\alpha_{E,lm}^{(j)}\boldsymbol{\Psi}_{lm}+\alpha_{B,lm}^{(j)}\boldsymbol{\Phi}_{lm}),\tag{1}$$

that allows us to represent it as light originated from a set of multipole emitters at the origin, with $l=1$ representing dipoles, $l=2$ quadrupoles, etc. However, while the magnetic coefficients $\alpha_{M,lm}$ are due to magnetic multipole sources with transverse current $\mathbf{r}\times\mathbf{J}\neq 0$, the electric coefficients $\alpha_{E,lm}$ can arise from two different types of polarization; electric and toroidal multipoles. These contributions can be calculated directly from the induced polarizations. Taking atom $j$ to be fixed at position $\mathbf{r}_j$, the induced displacement current density is $J_\sigma(\mathbf{r})=-i\omega\mathcal{D}\sum_j\mathcal{P}_\sigma^{(j)}\delta(\mathbf{r}-\mathbf{r_j})$. Inserting this in the standard multipole decomposition for an arbitrary distribution of currents [6] gives for the total electric and magnetic dipoles $\mathbf{d}=\sum_j\mathbf{d}_j$ and $\mathbf{m}=-(ik/2)\sum_j(\mathbf{r}_j\times\mathbf{d}_j)$, respectively, and for the toroidal dipole,

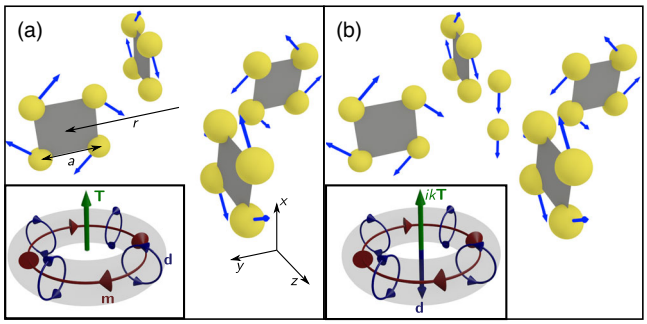


FIG. 1. (a) Geometry of a toroidal dipole unit cell consisting of a number of four-atom squares of width $a$, arranged in a circle of radius $r$, with atomic dipoles indicated by the arrows. A circulating electric polarization on the surface of a torus leads to magnetic dipoles forming a closed loop inside a torus (inset). These in turn contribute to a toroidal dipole moment through the center of the entire unit cell. (b) Geometry of an anapole unit cell. Adding two atoms to the center with induced dipole moments in the $x$ direction generates an electric dipole which destructively interferes with the toroidal dipole (inset).

$$\mathbf{T}=-\frac{ik}{10}\sum_j[(\mathbf{r}_j\cdot\mathbf{d}_j)\mathbf{r}_j-2\mathbf{r}_j^2\mathbf{d}_j].\tag{2}$$

The magnitude of the far-field electric dipole component, $|\alpha_{E,1}|\equiv[\sum_m|\alpha_{E,1m}|^2]^{1/2}\propto k^2|\mathbf{p}|/(4\pi\epsilon_0)$ then depends on the combination $\mathbf{p}=\mathbf{d}+ik\mathbf{T}$ [22]. We have checked that in our numerics corrections beyond the long-wavelength approximation of Eq. (1) are negligible.

We now turn to the design and preparation of a collective toroidal dipole. Even for atoms exhibiting electric dipole transitions, their collective excitation eigenmodes can be utilized in synthesizing radiative excitations, e.g., with magnetic properties [73,77]. The toroidal dipole, as illustrated in the inset of Fig. 1(a), consists of a poloidal electric current wound around a torus, such that magnetic dipoles form a closed loop, reminiscent of vortex current, pointing along a ring around the center of the torus. We approximate this geometry using squares of four atoms [see Fig. 1(a)]. This is possible, since an isolated square has a collective excitation eigenmode with the dipoles oriented tangentially to the center of the square [73]. While electric dipoles of the atoms average to zero on each square, they generate a magnetic dipole moment normal to the plane of the square.

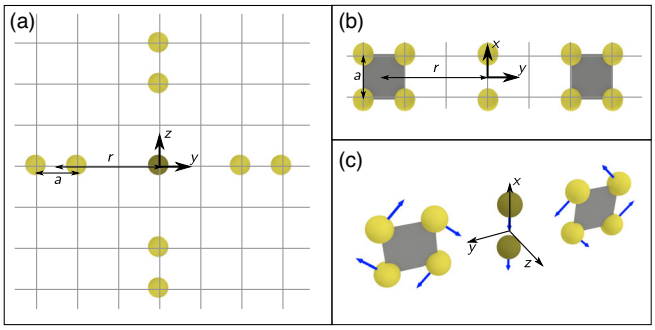


FIG. 2. Projections of geometry of toroidal dipole and anapole unit cells in (a) the $yz$ and (b) the $xy$ plane. Shaded atoms at $y$, $z = 0$ are absent for toroidal dipole unit cell but present for anapole unit cell. (c) Alternative structure for realizing a toroidal dipole or anapole excitation with all atoms in the $xy$ plane, the response of which is shown in Fig. S3 of Ref. [48].

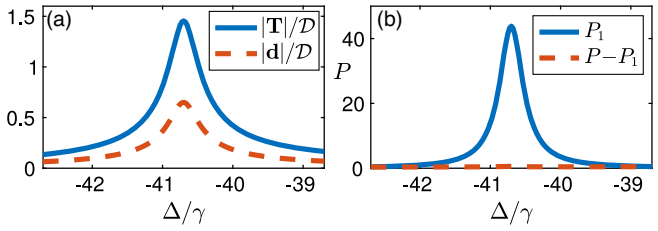


FIG. 3. Excitation of a toroidal dipole $\mathbf{T}$ as a multipole decomposition of (a) atomic dipoles [in dimensionless units of $\mathcal{D}\mathcal{E}_0/(\hbar\gamma)$]. (b) Far-field radiated power consisting of dipole contribution $P_1$ and the remaining power of all other contributions (in units of $I_{\text{in}}/k^2$, where $I_{\text{in}} = 2c\epsilon_0|\mathcal{E}_0|^2$ is the incoming intensity), as a function of the laser detuning from the atomic resonance, with $r = 0.2\lambda$ and $a = 0.08\lambda$, as defined in Fig. 1(a).

Arranging several of these squares in a circle, with each aligned perpendicular to the circumference, leads to the magnetic dipole moments winding around the center, as illustrated in the inset, creating a toroidal dipole pointing in the $x$ direction. The projections of this geometry in the $yz$ and $xy$ planes are shown in Figs. 2(a) and 2(b). A general choice of parameters could be realized with independent optical tweezers. However, in the case that $r = (n + 1/2)a$ for integer $n$, the ensemble could also be formed by selectively populating sites on a bilayer square lattice, as indicated by the gray grid.

We demonstrate this by an example calculation of four such squares, with $r = 0.2\lambda$ and $a = 0.08\lambda$ [Fig. 1(a)], resulting in altogether 48 collective excitation eigenmodes. This corresponds to a partially-populated bilayer square lattice with lattice constant $0.08\lambda$ [Figs. 2(a) and 2(b)]. We find a collective eigenmode exhibiting a strong toroidal dipole, with only a weak radiative coupling due to subradiant resonance linewidth $\upsilon = 0.2\gamma$. The scattered light from this eigenmode is dominated by $|\alpha_{E,1}|^2$ with >99% of the radiated power coming from this contribution, which can be decomposed locally into toroidal and electric dipoles with $|\mathbf{T}|/|\mathbf{d}| = 2.2$. At larger lattice spacings, the toroidal dipole contribution can get even more dominant.

To excite the toroidal dipole mode, we consider a plane wave propagating in the $x$ direction. The toroidal symmetry of the mode inhibits coupling to a drive field with uniform linear polarization. Instead, the symmetry can be matched by radial polarization $\hat{\mathbf{e}}_{\text{in}} = \hat{\mathbf{e}}_\rho$, where $\hat{\mathbf{e}}_\rho$ points outward in the $yz$ plane from the center of the toroidal dipole. The multipole decomposition of the local excitation in Fig. 3(a) displays a strong response of the toroidal dipole, as well as a weaker electric dipole response. Figure 3(b) shows the decomposition of the far-field power $P = 2c\epsilon_0 \int |\mathbf{E}|^2 dA$ integrated over a closed surface into the dominant dipole component $P_1 \propto |\alpha_{E,1}|^2$, which does not distinguish between contributions from $\mathbf{d}$ and $\mathbf{T}$, as well as the remaining sum of all other contributions. At the toroidal dipole resonance $\Delta = -40.7\gamma$ the occupation of the collective eigenmode is ≈99% [48].

Here we take four squares, distributed evenly on a ring around the center, to form the toroidal dipole moment, but similar results can be achieved with a minimum of only two. As illustrated in Fig. 2(c), with two squares centered at, e.g., $\pm r\hat{\mathbf{y}}$ having opposite chirality dipole orientation a toroidal dipole moment can also be achieved while all atoms lie in the single $xy$ plane [48].

We next consider a planar square lattice in the $yz$ plane with each unit cell as in Fig. 1(a). Because of radiative interactions, for a subwavelength-spaced lattice, the entire system responds as a coherent, collective entity, with delocalized collective excitation eigenmodes extending over the array. In particular, there is a collective eigenmode which corresponds to a uniform excitation of a toroidal dipole at each site. However, this mode cannot be excited by radially polarized light as it would require the symmetry to be broken around the center of each individual unit cell. Instead, we use uniform linear polarization, with $\hat{\mathbf{e}}_{\text{in}} = \hat{\mathbf{e}}_y$, but vary the atomic level shifts within each atom of the unit cell independently that are then repeated across the array on each unit cell. We numerically optimize the toroidal dipole moment on a single unit cell to calculate these level shifts.

The corresponding toroidal and electric dipole excitations are shown in Fig. 4(a). Despite the presence of the electric dipole, the toroidal dipole is the dominant component at $\Delta = -17\gamma$ where the ratio $|\mathbf{T}|/|\mathbf{d}| = 3.3$ is at its maximum. The dipole radiation is compared to the intensity of all other contributions to the scattered light in Fig. 4(b), showing that all other modes are also suppressed at this detuning.

This excitation closely corresponds to an eigenmode, delocalized across the entire array, consisting of a repetition of the poloidal dipole excitation on each unit cell, and forming an effective lattice of coherently oscillating toroidal dipoles. The linewidth of the collective mode [Fig. 4(c)] narrows strongly as the unit cell spacing decreases.

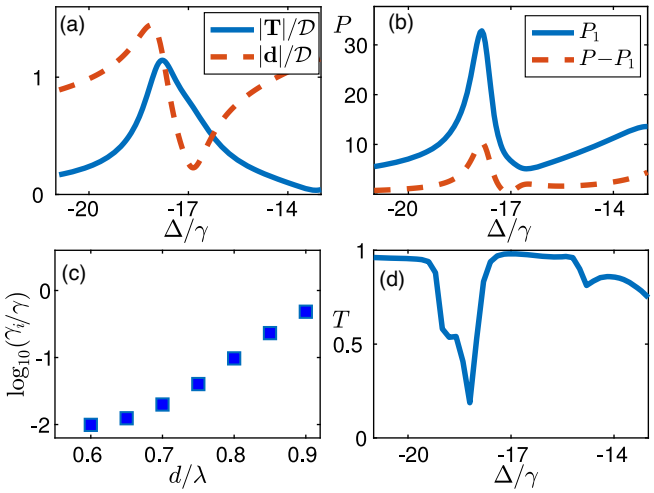


FIG. 4. Collective excitation of a $12 \times 12$ square array of toroidal dipole unit cells with spacing $d = 0.85\lambda$ ($a = 0.1\lambda$, $r = 0.2\lambda$). (a) Multipole decomposition of atomic dipoles [in units of $\mathcal{D}\mathcal{E}_0/(\hbar\gamma)$] for a single central unit cell, excited by linearly polarized light, (b) decomposition of the dipole contribution to the far-field radiated power, and the sum of all other contributions (in units of $I_{\text{in}}/k^2$), (c) collective linewidth $\upsilon$ of the uniform toroidal dipole eigenmode as a function of $d$, and (d) coherent transmission $T = |\mathbf{E}|^2/|\mathcal{E}_0|^2$ of light through the array, where $\mathbf{E}$ is the total field amplitude.

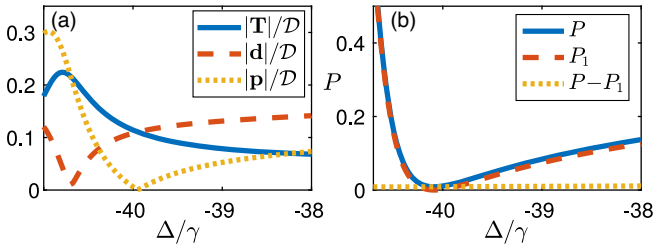


FIG. 5. Excitation of a nonradiating dynamic anapole, with a multipole decomposition of (a) atomic dipoles [in units of $\mathcal{D}\mathcal{E}_0/(\hbar\gamma)$], with $\mathbf{p} = \mathbf{d} + ik\mathbf{T}$, and (b) the far-field scattered light from all contributions, the total dipole component with intensity proportional to $|\mathbf{p}|^2$, and the sum of all other contributions (in units of $I_{\text{in}}/k^2$) as a function of the overall laser frequency detuning for $a = 0.08\lambda$, $r = 0.2\lambda$.

The transmitted light through the array can be calculated by adding the scattered light from each individual atom to the incoming light. At a positon $\zeta\hat{\mathbf{x}}$ from a uniform lattice of area $\mathcal{A}$, when $\lambda \lesssim \zeta \ll \sqrt{\mathcal{A}}$ the electric field of the light transmitted in the forward direction is given by [33,78–80]

$$\epsilon_0\mathbf{E} = \epsilon_0\mathcal{E}_0\hat{\mathbf{e}}_y e^{ik\zeta} + \frac{ik}{2\mathcal{A}}\sum_j [\mathbf{d}_j - \hat{\mathbf{e}}_x \cdot \mathbf{d}_j\hat{\mathbf{e}}_x]e^{ik(\xi - x_j)}. \quad (3)$$

The transmission $T = |\mathbf{E}|^2/|\mathcal{E}_0|^2$ shown in Fig. 4(d) displays narrow Fano resonances at the frequencies of toroidal and electric dipole excitations. (We note that a second dip at $\Delta = -15\gamma$ is due to coupling to an unrelated electric quadrupole mode.)

An especially fascinating configuration can be obtained by a combination of a toroidal and electric dipole forming a dynamic anapole. Because the far-field radiation of these dipoles is identical, they can destructively interfere such that the net radiation vanishes when $\mathbf{d} = -ik\mathbf{T}$. Despite having no emission, the anapole state has a nonzero energy, and a vector potential which cannot be fully eliminated by gauge transformation [19,81]. We show that the collective radiative excitations of strongly coupled atoms can form a dynamic anapole by adding a pair of atoms to the toroidal dipole configuration of Fig. 1(a), in the same bilayer planes of the existing atoms, that then synthesizes a coherent superposition of electric and toroidal dipoles [Fig. 1(b)]. The inset illustrates how the contribution of the electric dipole moment at the origin to the total dipole moment $\mathbf{p}$ points in the opposite direction to that of the toroidal dipole.

Again, we illustrate the case of four squares, distributed evenly on a ring around the center, but similar results can be achieved with a minimum of only two. As illustrated in Fig. 2(c), adding two central atoms at $\pm(a/2)\hat{\mathbf{x}}$, results in an anapole excitation while all atoms lie in the $xy$ plane [48].

The anapole can be excited by a radially polarized plane wave focused through a lens with high numerical aperture, leading to a longitudinal field in the $x$ direction along the beam axis which excites the central two atoms [48]. This field is calculated via the standard Richard-Wolf diffraction integral [82] with a numerical aperture of 0.7. The resulting multipole decomposition of atomic dipoles [Fig. 5(a)] displays a strong excitement of both the electric and toroidal dipole. However, the combination of these dipoles, $\mathbf{p} = \mathbf{d} + ik\mathbf{T}$, is much weaker. The total scattered intensity, along with the decomposition into the dipole contribution and that of all other multipoles, is shown in Fig. 5(b), indicating a near total cancellation of the scattered light.

In conclusion, we have shown how strong light-mediated dipolar interactions between atoms can be harnessed to engineer collective radiative excitations that synthesize an effective dynamic toroidal dipole or anapole. In both cases the toroidal topology is generated by radiative transitions forming an effective poloidal electric current wound around a torus. In a large lattice we show how to engineer a collective strongly subradiant eigenmode consisting of an effective periodic lattice of toroidal dipoles that exhibits a narrow Fano transmission resonance.

Data used in this publication is available at [83].

We acknowledge financial support from Engineering and Physical Sciences Research Council (Grants No. EP/S002952/1 and No. EP/P026133/1).

*k.ballantine@lancaster.ac.uk
†j.ruostekoski@lancaster.ac.uk

[1] J. D. Jackson, *Classical Electrodynamics*, 3rd ed. (Wiley, New York, 1999).
[2] R. E. Raab, O. L. De Lange, and O. L. de Lange, *Multipole Theory in Electromagnetism: Classical, Quantum, and Symmetry Aspects, with Applications* (Oxford University Press on Demand, Oxford, 2005), Vol. 128.
[3] N. Papasimakis, V. A. Fedotov, V. Savinov, T. A. Raybould, and N. I. Zheludev, Electromagnetic toroidal excitations in matter and free space, Nat. Mater. **15**, 263 (2016).
[4] N. Talebi, S. Guo, and P. A. van Aken, Theory and applications of toroidal moments in electrodynamics: Their emergence, characteristics, and technological relevance, Nanophotonics **7**, 93 (2018).
[5] V. M. Dubovik and V. V. Tugushev, Toroid moments in electrodynamics and solid-state physics, Phys. Rep. **187**, 145 (1990).
[6] C. Vrejoiu, Electromagnetic multipoles in Cartesian coordinates, J. Phys. A **35**, 9911 (2002).
[7] I. B. Zel Dovich, Electromagnetic interaction with parity violation, Sov. Phys. JETP **6**, 1184 (1958).
[8] V. F. Dmitriev and I. B. Khriplovich, P and T odd nuclear moments, Phys. Rep. **391**, 243 (2004).
[9] V. V. Flambaum and D. W. Murray, Anapole moment and nucleon weak interactions, Phys. Rev. C **56**, 1641 (1997).
[10] C. S. Wood, S. C. Bennett, D. Cho, B. P. Masterson, J. L. Roberts, C. E. Tanner, and C. E. Wieman, Measurement of parity nonconservation and an anapole moment in cesium, Science **275**, 1759 (1997).
[11] H. Schmid, On ferrotoroidics and electrotoroidic, magnetotoroidic and piezotoroidic effects*, Ferroelectrics **252**, 41 (2001).
[12] V. Savinov, V. A. Fedotov, and N. I. Zheludev, Toroidal dipolar excitation and macroscopic electromagnetic properties of metamaterials, Phys. Rev. B **89**, 205112 (2014).
[13] T. Kaelberer, V. A. Fedotov, N. Papasimakis, D. P. Tsai, and N. I. Zheludev, Toroidal dipolar response in a metamaterial, Science **330**, 1510 (2010).
[14] B. Ögüt, N. Talebi, R. Vogelgesang, W. Sigle, and P. A. Van Aken, Toroidal plasmonic eigenmodes in oligomer nanocavities for the visible, Nano Lett. **12**, 5239 (2012).
[15] Z.-G. Dong, J. Zhu, J. Rho, J.-Q. Li, C. Lu, X. Yin, and X. Zhang, Optical toroidal dipolar response by an asymmetric double-bar metamaterial, Appl. Phys. Lett. **101**, 144105 (2012).
[16] Y. Fan, Z. Wei, H. Li, H. Chen, and C. M. Soukoulis, Low-loss and high-$Q$ planar metamaterial with toroidal moment, Phys. Rev. B **87**, 115417 (2013).
[17] A. A. Basharin, M. Kafesaki, E. N. Economou, C. M. Soukoulis, V. A. Fedotov, V. Savinov, and N. I. Zheludev, Dielectric Metamaterials with Toroidal Dipolar Response, Phys. Rev. X **5**, 011036 (2015).
[18] D. W. Watson, S. D. Jenkins, J. Ruostekoski, V. A. Fedotov, and N. I. Zheludev, Toroidal dipole excitations in metamolecules formed by interacting plasmonic nanorods, Phys. Rev. B **93**, 125420 (2016).
[19] G. N. Afanasiev and Yu P. Stepanovsky, The electromagnetic field of elementary time-dependent toroidal sources, J. Phys. A **28**, 4565 (1995).
[20] V. Savinov, N. Papasimakis, D. P. Tsai, and N. I. Zheludev, Optical anapoles, Commun. Phys. **2**, 69 (2019).
[21] V. A. Fedotov, A. V. Rogacheva, V. Savinov, D. P. Tsai, and N. I. Zheludev, Resonant transparency and non-trivial non-radiating excitations in toroidal metamaterials, Sci. Rep. **3**, 1 (2013).
[22] A. E. Miroshnichenko, A. B. Evlyukhin, Y. F. Yu, R. M. Bakker, A. Chipouline, A. I. Kuznetsov, B. Luk'yanchuk, B. N. Chichkov, and Y. S. Kivshar, Nonradiating anapole modes in dielectric nanoparticles, Nat. Commun. **6**, 8069 (2015).
[23] S. D. Jenkins and J. Ruostekoski, Controlled manipulation of light by cooperative response of atoms in an optical lattice, Phys. Rev. A **86**, 031602(R) (2012).
[24] J. Perczel, J. Borregaard, D. E. Chang, H. Pichler, S. F. Yelin, P. Zoller, and M. D. Lukin, Photonic band structure of two-dimensional atomic lattices, Phys. Rev. A **96**, 063801 (2017).
[25] R. J. Bettles, S. A. Gardiner, and C. S. Adams, Cooperative ordering in lattices of interacting two-level dipoles, Phys. Rev. A **92**, 063822 (2015).
[26] G. Facchinetti, S. D. Jenkins, and J. Ruostekoski, Storing Light with Subradiant Correlations in Arrays of Atoms, Phys. Rev. Lett. **117**, 243601 (2016).
[27] S.-M. Yoo and S. M. Paik, Cooperative optical response of 2D dense lattices with strongly correlated dipoles, Opt. Express **24**, 2156 (2016).
[28] A. Asenjo-Garcia, M. Moreno-Cardoner, A. Albrecht, H. J. Kimble, and D. E. Chang, Exponential Improvement in Photon Storage Fidelities Using Subradiance and Selective Radiance in Atomic Arrays, Phys. Rev. X **7**, 031024 (2017).
[29] M. Hebenstreit, B. Kraus, L. Ostermann, and H. Ritsch, Subradiance via Entanglement in Atoms with Several Independent Decay Channels, Phys. Rev. Lett. **118**, 143602 (2017).
[30] V. Mkhitaryan, L. Meng, A. Marini, and F. J. de Abajo, Lasing and Amplification from Two-Dimensional Atom Arrays, Phys. Rev. Lett. **121**, 163602 (2018).
[31] E. Shahmoon, D. S. Wild, M. D. Lukin, and S. F. Yelin, Cooperative Resonances in Light Scattering from Two-Dimensional Atomic Arrays, Phys. Rev. Lett. **118**, 113601 (2017).
[32] P.-O. Guimond, A. Grankin, D. V. Vasilyev, B. Vermersch, and P. Zoller, Subradiant Bell States in Distant Atomic Arrays, Phys. Rev. Lett. **122**, 093601 (2019).
[33] J. Javanainen and R. Rajapakse, Light propagation in systems involving two-dimensional atomic lattices, Phys. Rev. A **100**, 013616 (2019).
[34] R. J. Bettles, M. D. Lee, S. A. Gardiner, and J. Ruostekoski, Quantum and nonlinear effects in light transmitted through planar atomic arrays, arXiv:1907.07030.
[35] C. Qu and A. M. Rey, Spin squeezing and many-body dipolar dynamics in optical lattice clocks, Phys. Rev. A **100**, 041602(R) (2019).
[36] K. E. Ballantine and J. Ruostekoski, Subradiance-protected excitation spreading in the generation of collimated photon emission from an atomic array, Phys. Rev. Research **2**, 023086 (2020).
[37] J. Rui, D. Wei, A. Rubio-Abadal, S. Hollerith, J. Zeiher, D. M. Stamper-Kurn, C. Gross, and I. Bloch, A subradiant

optical mirror formed by a single structured atomic layer, Nature (London) **583**, 369 (2020).
[38] Y. Wang, S. Subhankar, P. Bienias, M. Lacki, T.-C. Tsui, M. A. Baranov, A. V. Gorshkov, P. Zoller, J. V. Porto, and S. L. Rolston, Dark State Optical Lattice with a Subwavelength Spatial Structure, Phys. Rev. Lett. **120**, 083601 (2018).
[39] B. Olmos, D. Yu, Y. Singh, F. Schreck, K. Bongs, and I. Lesanovsky, Long-Range Interacting Many-Body Systems with Alkaline-Earth-Metal Atoms, Phys. Rev. Lett. **110**, 143602 (2013).
[40] B. J. Lester, N. Luick, A. M. Kaufman, C. M. Reynolds, and C. A. Regal, Rapid Production of Uniformly Filled Arrays of Neutral Atoms, Phys. Rev. Lett. **115**, 073003 (2015).
[41] T. Xia, M. Lichtman, K. Maller, A. W. Carr, M. J. Piotrowicz, L. Isenhower, and M. Saffman, Randomized Benchmarking of Single-Qubit Gates in a 2D Array of Neutral-Atom Qubits, Phys. Rev. Lett. **114**, 100503 (2015).
[42] M. Endres, H. Bernien, A. Keesling, H. Levine, E. R. Anschuetz, A. Krajenbrink, C. Senko, V. Vuletic, M. Greiner, and M. D. Lukin, Atom-by-atom assembly of defect-free one-dimensional cold atom arrays, Science **354**, 1024 (2016).
[43] D. Barredo, S. de Léséleuc, V. Lienhard, T. Lahaye, and A. Browaeys, An atom-by-atom assembler of defect-free arbitrary two-dimensional atomic arrays, Science **354**, 1021 (2016).
[44] H. Kim, W. Lee, H.-g. Lee, H. Jo, Y. Song, and J. Ahn, In situ single-atom array synthesis using dynamic holographic optical tweezers, Nat. Commun. **7**, 13317 (2016).
[45] A. Cooper, J. P. Covey, I. S. Madjarov, S. G. Porsev, M. S. Safronova, and M. Endres, Alkaline-Earth Atoms in Optical Tweezers, Phys. Rev. X **8**, 041055 (2018).
[46] A. Glicenstein, S. G. Ferioli, N. L. Brossard, I. Ferrier-Barbut, and A. Browaeys, Collective Shift of Resonant Light Scattering by a One-Dimensional Atomic Chain, Phys. Rev. Lett. **124**, 253602 (2020).
[47] R. H. Dicke, Coherence in spontaneous radiation processes, Phys. Rev. **93**, 99 (1954).
[48] See Supplemental Material at http://link.aps.org/supplemental/10.1103/PhysRevLett.125.063201 for technical details, which includes Refs. [1,3,26,36–42,45,49–72].
[49] J. Ruostekoski and J. Javanainen, Quantum field theory of cooperative atom response: Low light intensity, Phys. Rev. A **55**, 513 (1997).
[50] J. Javanainen, J. Ruostekoski, B. Vestergaard, and M. R. Francis, One-dimensional modeling of light propagation in dense and degenerate samples, Phys. Rev. A **59**, 649 (1999).
[51] M. D. Lee, S. D. Jenkins, and J. Ruostekoski, Stochastic methods for light propagation and recurrent scattering in saturated and nonsaturated atomic ensembles, Phys. Rev. A **93**, 063803 (2016).
[52] S. D. Jenkins, J. Ruostekoski, J. Javanainen, S. Jennewein, R. Bourgain, J. Pellegrino, Y. R. P. Sortais, and A. Browaeys, Collective resonance fluorescence in small and dense atom clouds: Comparison between theory and experiment, Phys. Rev. A **94**, 023842 (2016).
[53] A. A. Svidzinsky, J.-T. Chang, and M. O. Scully, Cooperative spontaneous emission of $n$ atoms: Many-body eigenstates, the effect of virtual Lamb shift processes, and analogy with radiation of $n$ classical oscillators, Phys. Rev. A **81**, 053821 (2010).
[54] E. A. Power and S. Zienau, Coulomb gauge in non-relativistic quantum electro-dynamics and the shape of spectral lines, Phil. Trans. R. Soc. A **251**, 427 (1959).
[55] R. G. Woolley, Molecular quantum electrodynamics, Proc. R. Soc. A **321**, 557 (1971).
[56] C. Cohen-Tannaudji, J. Dupont-Roc, and G. Grynberg, *Photons and Atoms: Introduction to Quantum Electrodynamics* (John Wiley & Sons, New York, 1989).
[57] R. H. Lehmberg, Radiation from an $n$-atom system. I. General formalism, Phys. Rev. A **2**, 883 (1970).
[58] D. W. Watson, S. D. Jenkins, V. A. Fedotov, and J. Ruostekoski, Point-dipole approximation for small systems of strongly coupled radiating nanorods, Sci. Rep. **9**, 5707 (2019).
[59] R. Alaee, C. Rockstuhl, and I. Fernandez-Corbaton, An electromagnetic multipole expansion beyond the long-wavelength approximation, Opt. Commun. **407**, 17 (2018).
[60] A. Alù and N. Engheta, Dynamical theory of artificial optical magnetism produced by rings of plasmonic nanoparticles, Phys. Rev. B **78**, 085112 (2008).
[61] A. B. Evlyukhin, C. Reinhardt, A. Seidel, B. S. Luk'yanchuk, and B. N. Chichkov, Optical response features of Si-nanoparticle arrays, Phys. Rev. B **82**, 045404 (2010).
[62] S. D. Jenkins and J. Ruostekoski, Theoretical formalism for collective electromagnetic response of discrete metamaterial systems, Phys. Rev. B **86**, 085116 (2012).
[63] S. D. Jenkins and J. Ruostekoski, Metamaterial Transparency Induced by Cooperative Electromagnetic Interactions, Phys. Rev. Lett. **111**, 147401 (2013).
[64] O. Morsch and M. Oberthaler, Dynamics of Bose-Einstein condensates in optical lattices, Rev. Mod. Phys. **78**, 179 (2006).
[65] U. Schnorrberger, J. D. Thompson, S. Trotzky, R. Pugatch, N. Davidson, S. Kuhr, and I. Bloch, Electromagnetically Induced Transparency and Light Storage in an Atomic Mott Insulator, Phys. Rev. Lett. **103**, 033003 (2009).
[66] J. F. Sherson, C. Weitenberg, M. Endres, M. Cheneau, I. Bloch, and S. Kuhr, Single-atom-resolved fluorescence imaging of an atomic Mott insulator, Nature (London) **467**, 68 (2010).
[67] C. Weitenberg, M. Endres, J. F. Sherson, M. Cheneau, P. Schauß, T. Fukuhara, I. Bloch, and S. Kuhr, Single-spin addressing in an atomic Mott insulator, Nature (London) **471**, 319 (2011).
[68] R. P. Anderson, D. Trypogeorgos, A. Valdés-Curiel, Q.-Y. Liang, J. Tao, M. Zhao, T. Andrijauskas, G. Juzeliunas, and I. B. Spielman, Realization of a deeply subwavelength adiabatic optical lattice, Phys. Rev. Research **2**, 013149 (2020).
[69] S. Nascimbene, N. Goldman, N. R. Cooper, and J. Dalibard, Dynamic Optical Lattices of Subwavelength Spacing for Ultracold Atoms, Phys. Rev. Lett. **115**, 140401 (2015).
[70] M. Lacki, P. Zoller, and M. A. Baranov, Stroboscopic painting of optical potentials for atoms with subwavelength resolution, Phys. Rev. A **100**, 033610 (2019).
[71] D. Barredo, S. de Léséleuc, V. Lienhard, T. Lahaye, and A. Browaeys, An atom-by-atom assembler of

defect-free arbitrary two-dimensional atomic arrays, Science **354**, 1021 (2016).

[72] F. Gerbier, A. Widera, S. Fölling, O. Mandel, and I. Bloch, Resonant control of spin dynamics in ultracold quantum gases by microwave dressing, Phys. Rev. A **73**, 041602(R) (2006).

[73] K. E. Ballantine and J. Ruostekoski, Optical magnetism and Huygens' surfaces in arrays of atoms induced by cooperative responses, arXiv:2002.12930.

[74] O. Morice, Y. Castin, and J. Dalibard, Refractive index of a dilute Bose gas, Phys. Rev. A **51**, 3896 (1995).

[75] I. M. Sokolov, D. V. Kupriyanov, and M. D. Havey, Microscopic theory of scattering of weak electromagnetic radiation by a dense ensemble of ultracold atoms, J. Exp. Theor. Phys. **112**, 246 (2011).

[76] The light and atomic polarization amplitudes here refer to the slowly varying positive frequency components, where the rapid variations $\exp(-i\omega t)$ at the laser frequency have been factored out.

[77] R. Alaee, B. Gurlek, M. Albooyeh, D. Martin-Cano, and V. Sandoghdar, Quantum metamaterials with magnetic response at optical frequencies, arXiv:2002.03385 [Phys. Rev. Lett. (to be published)].

[78] L. Chomaz, L. Corman, T. Yefsah, R. Desbuquois, and J. Dalibard, Absorption imaging of a quasi-two-dimensional gas: A multiple scattering analysis, New J. Phys. **14**, 055001 (2012).

[79] J. Javanainen, J. Ruostekoski, Y. Li, and S.-M. Yoo, Exact electrodynamics versus standard optics for a slab of cold dense gas, Phys. Rev. A **96**, 033835 (2017).

[80] G. Facchinetti and J. Ruostekoski, Interaction of light with planar lattices of atoms: Reflection, transmission, and cooperative magnetometry, Phys. Rev. A **97**, 023833 (2018).

[81] N. A. Nemkov, A. A. Basharin, and V. A. Fedotov, Nonradiating sources, dynamic anapole, and Aharonov-Bohm effect, Phys. Rev. B **95**, 165134 (2017).

[82] B. Richards and E. Wolf, Electromagnetic diffraction in optical systems. II. Structure of the image field in an aplanatic system, Proc. R. Soc. A **253**, 358 (1959).

[83] https://doi.org/10.17635/lancaster/researchdata/377.